RSC Advances




ROYAL SOCIETY OF CHEMISTRY

www.rsc.org/advances

# Development and Characterization of Single Step Self-Assembled Lipid Polymer Hybrid Nanoparticles for Effective Delivery of Methotrexate

Neeraj K. Garg[1], Bhupinder Singh[1, 2], Gajanand Sharma[1, 3], Varun Kushwah[4], Rajeev K. Tyagi[5, #], Sanyog Jain[4], Om Prakash Katare[1]*

[1]*Drug Delivery Research Group, University Institute of Pharmaceutical Sciences, UGC Centre of Advanced Studies, Panjab University, Chandigarh 160014, India*

[2]*UGC-Centre of Excellence in Applications of Nanomaterials, Nanoparticles &Nanocomposites (Biomedical Sciences), Panjab University, Chandigarh 160 014, India*

[3]*Formulation Research, Ipca Laboratories Limited, Kandivli Industrial Estate Ltd., Kandivli (W), Mumbai, Maharashtra, India 400 067.*

[4]*Centre for Pharmaceutical Nanotechnology, Department of Pharmaceutics, National Institute of Pharmaceutical Education and Research (NIPER), Sector 67, SAS Nagar (Mohali), Punjab 160062, India*

[5]*Department of Periodontics, College of Dental Medicine Georgia Regents University, Augusta, Georgia 30912, USA*

---

***To whom correspondence should be addressed**
Dr Om Prakash Katare
M Pharm, Ph D
Professor of Pharmaceutical Sciences
Division of Pharmaceutics
University Institute of Pharmaceutical Sciences
UGC-Centre of Advanced Study
Panjab University, Chandigarh 160 014, India
E-mail: drkatare@yahoo.com, katare@pu.ac.in

**# Current address:** Biosafety Support Unit, Regional Centre for Biotechnology-DBT, C.G.O. Complex, Lodhi Road, New Delhi-110003, India.

**Abstract**

The present study was designed to develop methotrexate (MTX) loaded lipid polymer hybrid nanoparticles (LPHNPs) for spatial and controlled delivery of this drug. LPHNPs were formulated by single step self-assembled nano-precipitation method. The effect of variables such as surfactants, varying surfactant concentration, phospholipids and lipid-polymer ratio on particle size and drug entrapment efficiencies were systematically assessed to optimize LPHNPs. The formulated LPHNPs were found in nanometric size range (150-300) with spherical shape. The entrapment efficiency of developed formulations was calculated between 80-90%. The entrapment of drug into nanoparticles was further validated by FTIR and XRD analysis. *In vitro* drug release study showed slow and sustained drug release i.e. more than 80% at the end of $7^{th}$day. The drug release followed Korsmeyer-Peppas model showing Fickian diffusion. The *in-vitro* cytotoxicity of optimized formulations was assessed in MCF-7 cells by MTT, immunofluorescence assay (IFA) as well as confocal laser scanning microscopy (CLSM). The result obtained with *in vitro* cell line studies suggested that LPHNP is a prominent delivery vehicle for MTX in breast cancers.

**Key Words:** Lipid polymer hybrid nanoparticles (LPHNPs); Methotrexate; Cancer targeting; Single step method; MCF-7 cell lines; Immunofluorescence assay (IFA); Phospholipids; Lutrol® F-87; Kolliphor® P 407.

## 1. Introduction

Lipid polymer hybrid nanoparticles (LPHNPs) have emerged as a promising drug delivery system to exploit the drug carrier potential of liposomes and polymeric nanoparticles (NPs) and to overcome their limitations. This delivery arrangement addresses the limitations, such as low solubility, dose-related toxicity, non-specificity, rapid diffusion throughout the body, short half-life in bloodstream, and development of drug-resistance of conventional lipid and polymer based NPs by target cell[1]. These properties of LPHNPs are indicative of their utility and prove advantageous over existing delivery vehicles[1]. Further, lipid layer slows down the rate of polymer degradation of LPNs product by limiting inward water diffusion, and therefore accounts for sustained release kinetics of loaded content[2]. Thus, well-designed hybrid lipid–polymer nanoparticle contains hydrophobic polymeric core functions, whereas the surrounding lipid coat functions as (i) a biocompatible shield (ii) a barrier preventing fast leakage of water-soluble drugs [3,4]. The properties such as biocompatibility, biodegradability, sustained drug-release profiles, and greater loading capacity attribute to stable, high-payload targeted drug delivery vehicle that can maximize chemotherapeutic efficacy against targeted cancer cells[5].

MTX, a folate antagonist, is a widely used for the treatment of many forms of cancer, including brain tumor, breast and ovarian cancer, several leukemias[6]. However, its usage is limited due to its low-solubility, dose-related cytotoxicity, non-specific rapid diffusion throughout the body, short half-life in bloodstream, and development of resistance by target cells[7,8]. Various drug delivery carriers including solid lipid nanoparticles (SLNs)[9], nanostructured lipid carriers[10] (NLCs), polymeric NPs[11,12], and liposomes[13,14] have been used to address these issues. Although these delivery vehicles showed their value in disease therapeutics, there are some obvious constraints with these carriers. To mention a few are a) liposomes get cleared from Reticulo-endothelial System (RES), b) They lack in structural integrity and stability[15], c) drug crystallization, and polymorphic changes in SLNs upon storage. To overcome these limitations of lipid and polymeric NPs, LPHNPs are preferred. LPHNPs have been used for the delivery of various chemotherapeutic agents such as docetaxel, paclitaxel-cisplatin, paclitaxel, gemcitabine etc. and also the delivery of siRNA[16,17] mRNA, DNA and proteins to tumor cells[2]. Recently

LPHNPs used for co delivery of siRNA and gemcitabine for pancreatic cancer therapy[16]. Despite numerous reports on LPHNPs in tumor-targeted delivery, the absence of well-defined MTX loaded LPHNPs has hampered the investigation of hybrid NPs on interactions with cancer cells. Keeping these facts in mind, MTX loaded LPHNPs were prepared.

The present study reports a single step self-assembled nanoprecipitation method of MTX encapsulated LPHNPs. Several variables like lipids, lipid/polymer ratio, surfactants and surfactant concentrations were tried to get particle size <200 nm, good PDI and maximum entrapment of MTX. The developed and optimized system showed significant *($p<0.05$)* anticancer and cellular uptake efficacy. To best of our knowledge, this study is the first attempt, to show the preparation of MTX-loaded LPHNPs for breast cancer therapy and might prove effective for the treatment of other cancers.

## 2. Materials and Methods

### 2.1 Materials

MTX and Lipoid SPC-3 (L-SPC-3) were obtained as kind samples from IPCA, Pvt. Ltd., Mumbai, India and M/s VAV-Life Sciences Pvt., Ltd, Mumbai, India respectively. Phospholipon 90G (PL-90G) and Phospholipon-S100 (PL-S100) were obtained as kind gift from Lipoid GmbH, Ludwigshafen, Germany. Polycaprolactone (PCL) (MW~14,000, Mn~10,000) was procured from Sigma-Aldrich, Chemical Co. (St. Louis, MO, USA). Lutrol® F-87 and Kolliphor® P-407 were provided as gift samples from BASF, Mumbai, India. Tween 80 and DMF were procured from Thermo Fisher Scientific India Pvt. Ltd, Mumbai, India and Central Drug House, New Delhi, India, respectively. All other chemicals and reagents are of analytical grade, solvents used for HPLC were of HPLC grade.

### 2.2 Methods

#### 2.2.1 Preparation of LPHNPs

MTX loaded LPHNPs (MTX-LPHNPs) were prepared by single step nanoprecipitation method[18]. Briefly, MTX, phospholipid and PCL were dissolved in 5 mL DMF. This solution was added drop

wise into surfactant solution by using 1mL syringe with constant flow rate at 1mL/min. Solution was kept for stirring on magnetic stirrer (Remi, Mumbai, India) at 800 rpm for 2-3 h. The organic phase was then removed by dialysis (MW 10 KD, Himedia, Mumbai) against the double distilled water for 12 h[18]. PCL-NPs were also prepared by using exactly same method as described above except phospholipid was excluded from the process. The optimized NPs were lyophilized (Vir Tis, Wizard 2.0, New York, U.S.A.) by our previously developed and patented stepwise freeze-drying cycle[19]. The condenser temperature and pressure applied was -60 °C and 200 Torr respectively in each step of cycle. Mannitol (5% w/v) was used as a cryoprotectant.

**2.2.2 Characterization of LPHNPs**

The characterization of MTX-LPHNPs was done with respect to size, PDI, zeta potential, surface morphology and drug entrapment efficiency. Size and PDI of NPs were determined by dynamic light scattering, while zeta potential was determined on the basis of electrophoretic mobility under an electric field by using zeta sizer (Nano ZS, Malvern, U.K.)

The surface morphology of LPHNPs was evaluated by transmission electron microscopy (TEM). A drop of diluted LPHNPs suspension was placed on a membrane coated grid surface and immediately stained with a drop of 1% phosphotungstic acid. After 1 min excess fluid was removed and the grid was air dried and was examined under High Resolution Transmission Electron Microscope (HRTEM; Fei, Electron Optics).

Fourier Transform Infrared Spectroscopy (FTIR) measurements were carried out on a Perkin Elmer Spectrum (Version 10.03.08) spectrometer operated at a resolution of 4 $cm^{-1}$ in the range of 450–4000 $cm^{-1}$.

X-ray Diffraction (XRD) pattern of the NPs was recorded on X'PertPRO-PANalytical (Netherlands) Advanced X-ray diffractometer. Free drug, blank LPHNPs and MTX loaded LPHNPs were analyzed. A known amount of each sample (10-15 mg) was loaded in a 25 mm poly-methyl methacrylate (PMMA) holder. The diffracto-grams were analyzed with X'Pert high score software.

Drug entrapment efficiency was calculated by direct lysis method. Briefly, weighed amount of freeze dried LPHNPs was added to 5 mL DMF followed by brief sonication to lyse the particles. The mixture was then filtered and diluted suitably analyzed by HPLC (Shimadzu LC-2010 CHT) method previously developed and validated by our group[20]. Reversed phase C18 column (10µm, 4.6 mm×250 mm, Waters) was used for chromatographic separation. The mobile phase was a mixture of buffer (pH 6.0) and acetonitrile in the ratio of 9:1. Samples were analyzed at 1.2 mL/min flow rate and detected at 302 nm. Percentage drug encapsulation efficiency was calculated by using following equation.

$$\text{Entrapment Efficiency (\%)} = \frac{\text{Amount of drug entrapped in LPHNPs}}{\text{Total amount of drug added}} \times 100$$

**2.2.3 Optimization of composition/process variables for LPHNPs**

**2.2.3.1 Screening of stabilizers and suitable surfactant concentration**

The compositions/process variables were screened on the basis of particle size, PDI, zeta potential and entrapment efficiency. Different stabilizers viz. Tween 80, Lutrol® F-87, Kolliphor® P 407 and PVA were screened to identify most suitable surfactant for MTX loaded LPHNPS formulation.

After selecting the most suitable stabilizer, its optimum concentration required for the preparation of MTX-LPHNPs was determined by using different stabilizer concentrations (0.5%, 1% and 2 %), and observing their effects on size, and EE of LPHNPs.

**2.2.3.2 Screening of phospholipids and screening of lipid polymer ratio**

The developed LPHNPs were further optimized with respect to different phospholipids, lipid: polymer ratio. In this study effect of different phospholipids such as, PL- S100, PL- 90 G, L-SPC-3 and different lipid polymer ratios such as 1:2, 1:4, and 1:6 on the particle size, PDI, zeta potential and entrapment efficiencies were evaluated.

### 2.2.4 *In vitro* drug release

The *in vitro* drug release study of optimized formulations was performed in phosphate buffer saline (pH= 7.4) and acetate buffer saline (pH 5.4); both containing a small amount of DMF (in 5:1 ratio) to mimic the physiological and lysosomal pH, respectively by using dialysis bag method[20]. Briefly, a known amount of lyophilized LPHNPs (equivalent to 5 mg of drug) was dispersed in 2 mL of respective buffer) and put into dialysis bag. This dialysis bag was then immersed in 20 mL of release medium. Samples were withdrawn at regular time intervals and replaced with fresh medium to maintain sink conditions. Samples were analyzed by HPLC method and drug release was recorded.

*In vitro* drug release data were fitted to various kinetic models such as zero order, first order, Higuchi model, Hixon-Crowell model and Korsemeyer-Peppas model. The regression analysis was performed. The graphs of the respective models were plotted according to the need of each equation. The equation for each drug release model is given below [21]:

**a) Zero Order Release Kinetics:-**

$$Q = Q_0 + k_0 t,$$

Where Q is the amount of drug released or dissolved, $Q_0$ is the initial amount of drug in solution (which is usually zero), $k_0$ is the zero order release constant. The plot was made between Cumulative % drug release vs. time.

**b) First order release Kinetics:-**

$$\text{Log } C = \text{Log } C_0 - k_t/2.303$$

Where, $C_0$ is the initial concentration of drug and k is first order constant. The plot was made between log cumulative percent released vs. time.

**c) Hixson- Crowell release kinetics**

$$Q_0^{1/3} - Q_t^{1/3} = k_H C_t$$

Where, $Q_t$ is the amount of drug released in time t, $Q_0$ is the initial amount of the drug and $k_H C$ is the rate constant for Hixson- Crowell rate equation. The plot was made of cube root % remaining in matrix vs. time.

**d) Higuchi release kinetics**

Higuchi tried to relate the drug release rate to the physical constants based on simple laws of diffusion. Higuchi was the first to derive an equation to describe the release of drug from an insoluble matrix as the square root of a time dependent process.

$$Q_t = k_H(t)^{0.5}$$

Where, $Q_t$ is the amount of drug released in time t, $k_H$ is the rate constant. The plot was made of cumulative %drug release vs. square root of time.

**e) Korsmeyer-Peppas release kinetics**

$$Mt/Mo = kt_n$$

Where, Mt/Mo is a fraction of drug released at time t, k is the rate constant and n is the release exponent. The plot was made between % cumulative log percent permeated vs. log time.

### 2.2.5 Stability studies

The stability stabilities of LPHNPs involved short term observation of different characteristics, *viz*., physical appearance, particle size, PDI, zeta potential and appearance of drug crystals or precipitates. The NPs were evaluated according to ICH guidelines at three different storage conditions i.e. in refrigerated condition (2-8°C), room temperature (25±2°C/60±5%RH) and elevated temperature (40±2°C/75±5% RH) for a period of 3 months.

### 2.2.6 *In vitro* cell culture studies

#### 2.2.6.1 *In vitro* cell culture

MCF-7, human breast adenocarcinoma cells (ATCC, Manassas, VA, USA) were cultured and maintained as earlier reported[22]. In brief, MCF-7 cells were grown in tissue culture flasks and maintained under 5% $CO_2$ atmosphere at 37°C. The growth medium comprised of Minimum Essential Medium Eagle (MEM, Sigma) supplemented with Earle's salts, L-glutamine, nonessential amino acids, sodium bicarbonate, sodium pyruvate, 10% fetal bovine serum (FBS), 100 U/mL penicillin, and 100 µg/mL streptomycin (PAA Laboratories GmbH, Austria). The growth medium was changed on alternate day. The cultured salts were trypsinized once 90% confluent with 0.25% trypsin-EDTA solution (Sigma, USA). MCF-7 cells were seeded at a density of 10,000 cell/well and 50,000 cells/well in 96-well and6-well culture plate (Costars, Corning

Inc., NY, USA) for quantitative cell viability by MTT assay[23] and qualitative cell uptake analysis by CLSM respectively[22].

**2.2.6.2 Cell uptake**

The *in vitro* cell uptake study was done as with Coumarin-6 (C-6) fluorescent co encapsulated with MTX- LPHNPs. The coumarin-6 was added in the organic phase (DMF) and coumarin-6 co-encapsulated MTX-LPHNPs were prepared following the procedure as described in section 2.2.1.After the cells reached confluency, the medium was removed, and cells were washed at least three times with Hank's Buffered Salt Solution (HBSS) (PAA Laboratories GmbH, Austria). The cells were incubated with coumarin-6-MTX-LPHNPs (equivalent to 1 µg/mL free coumarin-6)for 3h and extracellular particles were removed by washing with HBSS (5x). The cells were fixed with 3% paraformaldehyde (Merck, India) and permeabilized with 0.2% Triton X-100 (Sigma, USA).The cells were observed under CLSM (Olympus FV1000, Japan) and photomicrograph was taken at suitable magnifications.

**2.2.6.3 Cell cytotoxicity**

The cell suspension was added in 96 well tissue culture plates (0.2 mL/well) and incubated overnight for cell attachment. Following attachment, the growth medium was replaced with complete medium (0.2 mL) containing the free MTX or MTX-LPHNPs (F3, F5 and F9)to the different wells so as to achieve net concentrations of 0, 0.1, 1, 10 and 20 µg/mL (equivalent to free MTX) for 24, 48 and 72 h. Following treatment and completion of particular time, the cells were washed with PBS, pH 7.4 followed by addition of 150 µL of MTT solution (0.5mg/mL in PBS) to each well and reincubation for 3−4 h to facilitate formation of formazan crystals. The excess solution was then aspirated carefully, and MTT formazan crystals were dissolved in 200 µL of DMSO. The optical density (OD) of the resultant solution was then measured at 550 nm using an ELISA plate reader (BioTek, USA) and cell viability was assessed[22].

**2.2.6.4 Immunofluorescence Assay (IFA)**

IFA was performed on cells aggregated on a glass slide using cytospin (Thermo Scientific). Briefly, cells were plated at 37$^{o}$C for 4 minutes at 1000 rpm onto slide by cytospin. The cell labeling with CMFDA (5-chloromethylfluorescein diacetate) was carried out according to manufacturer's recommendations (Life Technologies, USA). The cells were then fixed with 4% paraformaldehyde in PBS (10 min at room temperature) followed by three times washing in $dH_2O$ for 5 minutes each. The processed slides were mounted with fluorescence mounting medium (Vecta shield, Vector laboratories, CA, USA) and images were taken under a microscope (Nikon instruments).

**Statistical analysis**

Statistical analysis was carried out by Student's t-test using Prism software (Graph Pad 5 Demo) and data was expressed as the mean ± standard deviation (S.D.) of the mean. (*$p$< 0.05, **$p$< 0.01 and ***$p$< 0.001). A value of P < 0.05 was considered statistically significant.

## 3. Results and Discussion

### 3.1 Preparation and characterization of LPHNPs

In this study, hydrophilic surfactant stabilized phospholipid coated LPHNPs having hydrophobic polymeric core were prepared. All the materials used in NPs formulation were clinically safe and biodegradable. LPHNPs were prepared by single step nanoprecipitation method **(Scheme 1)**. Methotrexate was encapsulated in PCL hydrophobic core, while lipid and surfactant establishes self-assembled shell around MTX encapsulated PCL core.

**-Space for Scheme 1-**

### 3.2 Optimization of formulation variables

#### 3.2.1 Lipids and surfactants

LPHNPs were prepared by three different phospholipids in combination with four different surfactants (Table 1). During the initial optimization lipid: polymer ratio 1:2, and surfactant

concentration 0.5 % w/v were used. Different surfactants including Tween 80, Lutrol® F-87, Kolliphor® P 407, polyvinyl alcohol (PVA) were screened and their effect on formulation and its characteristic properties was assessed systematically. The phospholipids in combination with Lutrol® F-87 showed optimum results **(Table 1)**. It should be noted that Kolliphor® P 407 andLutrol®F-87 gave smallest particle size with highest entrapment, Lutrol®F-87, was rated the best amongst all.Lutrol®F-87 and Kolliphor® P-407 are the grades of poloxamer and are triblock copolymer of ethylene oxide (EO) and propylene oxide (PO), which helps to form self-assembled hydrophilic outer shell of lipid polymer surface. Consistent to reported earlier, we report that poloxamer enhances entrapment efficiency and reduces particle size of NPs at a given concentration[24]. Combination of Lutrol® F-87 andPL-S100 (F5) showed best entrapment amongst all formulation with particle size less than 200 nm, however, all three phospholipids based formulations (F3, F5 and F9) were selected to carry out further experiments to assess the effect of different phospholipids on their biological activity. The particle size and zeta potential of PCL nanoparticles prepared by the same procedure as F5 (by using Lutrol® F-87), was found to be 27±1.6 nm and -12mV respectively.

We could hardly see any significant difference ($p$>0.05) in NPs physicochemical properties before and after lyophilization with respect to particle size, zeta potential, PDI and entrapment efficiency (data not shown).

**-Space for Table 1-**

### 3.2.2 Surfactant concentration

The varying surfactant concentrations (0.5-2% w/v) have been used to achieve optimum size and greater entrapment efficiency of NPs. The increase in surfactant concentration led to decrease in NPs particle size and significant *(p<0.01)* decrease in entrapment efficiency **(Fig. 1a)**. This decrease in particle size may be attributed to increased diffusion of drug from droplets to external phase which in turn leads to the reduction in particle size. Consistent to earlier reports[25], we have also observed stability of small sized droplets and prevention of coalescence into bigger droplet. A marked effect of surfactant concentration on stability and coalescence of

smaller droplets into bigger ones has been seen with Lutrol® F-87.The greater number of surfactant molecules are oriented at organic solvent/water interface to reduce interfacial tension at higher surfactant concentration during the emulsification process and promoted formation of smaller emulsion droplets. However, higher concentration of surfactant would increase also partitioning of drug from internal to external phase which ultimately results in decrease in entrapment efficiency[26]. The effect of surfactant concentration on NPs characterizations are summarized in SI Table 1 and based on the observations 0.5%w/v concentration was chosen as optimum.

**-Space for Figure 1a-**

### 3.2.3. Lipid: polymer ratio

Different lipids and polymers ratio (1:6, 1:4 and 1:2) were used to optimize the characterization parameters of NPs **(Fig. 1b)**. A proportionate increase in entrapment efficiency with the increasing concentration of phospholipids was observed which in turn showed increased size of NPs. This increased entrapment efficiency is probably due to the prevention of leaching out of drug from polymeric matrix. The increased concentration of lipids tends to increase viscosity of medium and resulted into the rapid solidification. This solidification would further prevent drug diffusion to external phase of medium and leads to greater and speedy encapsulation of drug [27]. The details on the lipid ratio on the characterization of NPs have been tabulated **(SI Table 2)**.

**-Space for Figure 1b and SI Table 2-**

The lipid/polymer weight ratio results in NPs with favorable combination of size (75-300 nm), entrapment efficiency (64-90%) and zeta potential (-12 to -22 mV) for unlimited application of drug delivery[28]. It has been already reported when ratio oflipid to polymer is increased, the excess lipids (beyond the critical micellar concentration of phospholipid) resulted into assembly of vesicles[1]. Therefore, lipid: polymer ratio prompted shuttling of NPs in to the assembled phospholipid vesicle[29]. Thus, coexistence of these vesicles would enhance overall measured size of hybrid NPs and led to a decrease in their zeta potential. Further, lipid: polymer ratio is directly proportionate to the particle size. We reason that at this optimized ratio, amount of

lipids is in the range to be able to cover entire surface of PCL hydrophobic core[1], and dispersed individually with lipid coating as a consequence of which small particle size was resulted. Conversely, at the lower lipid: polymer ratio, the scarce amount of lipids are not enough to cover surface of PCL core, and therefore resulted in higher zeta potential (nearly similar to bare PCL NPs). Our results are in line with that reported earlier[4,29], We report, that polymeric NPs in vesicle/coating of a lipid monolayer may serve two different roles; (a) to abstain MTX from being diffused out of PCL NPs core, and thereby improving MTX encapsulation & loading yield, and (b) to reduce the water penetration rate into the PCL core, and therefore decreased rate of hydrolysis of PCL polymers prompting slower drug release out of NPs[1]. Based upon entrapment and drug loading efficacy, lipid/polymer hybrid NPs with 1:2 were opted to carry out experiments with all phospholipids.

### 3.3 X-Ray Diffraction

The XRD pattern of MTX showed characteristic crystalline peaks at various 2θ positions of $7.9^0$, $9.5^0$, $11.7^0$, $13.0^0$, $14.5^0$, $19.3^0$, $21.6^0$ and $28.0^0$. XRD pattern of blank LPHNPs showed the crystalline peaks only at $21.4^0$ and $23.8^0$, whereas XRD pattern of MTX-LPHNPs showed slight shifting of peak positions to blank LPHNPs at $21.6^0$ and $24.0^0$. Furthermore, we hardly saw any MTX peak in XRD pattern of MTX-LPHNPs **(Fig. 2A a)**, which indicates the encapsulation of MTX in the NPs.

### 3.4 Fourier Transform Infrared (FTIR)

FTIR spectra of MTX, plain LPHNPs and MTX-LPHNPs are shown in **Fig. 2A b**. The characteristic peaks of MTX are observed at 828 $cm^{-1}$, 986 $cm^{-1}$,1243 $cm^{-1}$ , 1495 $cm^{-1}$ 1645 $cm^{-1}$, 2932 $cm^{-1}$, and 3290 $cm^{-1}$, and characteristic peaks of plain LPHNPs are observed at 962 $cm^{-1}$, 1239 $cm^{-1}$, 1365$cm^{-1}$, 1462$cm^{-1}$, 1728$cm^{-1}$, 2923 $cm^{-1}$. The characteristic peaks of MTX by MTX loaded LPHNPs were observed with slight shifting at 1242 $cm^{-1}$, 1367$cm^{-1}$ 1647 $cm^{-1}$and 2926 $cm^{-1.}$ These results are confirmatory of MTX loading onto LPHNPs.

**-Space for Figure 2A-**

### 3.5 Surface morphology

We report to achieve spherical shape and nanometric size of both NPs (polymeric and LPHNPs). A comparative analysis of LPHNPs on TEM images of polymeric NPs (PCL-NPs) **(Fig. 2B a)** has been done and shown to have achieved size less than 25 nm compared to LPHNs **(Fig. 2B b)** showing size > 50 nm. We found another striking difference of LPHNPs with different small, black and dense spherical bodies covered under lipid coating which might be PCL-NPs.

**-Space for Figure 2B -**

### 3. 6 *In vitro* drug release

Intracellular milieu is pretty complex because differential pH and chemo-enzymatic conditions prevailing indifferent intracellular compartments. For example, cytosolic pH is neutral to slightly alkaline (7.4−7.8) and lysosomal pH is acidic (4−5.5)[23,30]. As wide variety of cellular proteases and esterase are present in cellular compartments, activity of these enzymes critically dependent upon chemical constitution of substrate. It will be particularly beneficial if carrier-bound drug is localized in cytoplasm because drug molecule will be released rapidly at cytosolic pH. Furthermore, formulation showing faster release rate under acidic condition might take advantage of carrier-drug combination localized in lysosomes. As evident from **Fig. 3**, drug release from LPHNPs dependent upon pH and/or solubility of the drug in the given medium.

**-Space for Figure 3-**

All three formulations showed nearly same drug release pattern, however % cumulative drug release varied case by case. The formulations showed biphasic, slow and sustained release for 7 days (168 h). The drug release calculated during first 4 h was 15-35% at acidic pH (5.4) with all formulations, however, F5 and F9 showed highest drug release i.e., ~33% and ~29%. Approximately 65% MTX released from NPs during 72 h incubation at physiological pH (7.4) , and 70−80% drug release was observed at pH 5.4, and then sustained release upto7 consecutive days was seen. This suggests the greater release of MTX in acidic ambience of tumor as compared to that seen with normal tissues. This pH dependent release behavior is

advantageous during cellular internalization of LPHNPs which leads to the tracing and trafficking towards lysosomes. This lower pH environment helps lysosomes augmenting drug release within acidic tumor endosomes[30]. We observed impact of particle size on %age cumulative release from formulated NPs. Therefore, F5 with least particle size (below 200 nm) showed greater drug release, against F9 with greatest particle size (~250nm) and showing slowest drug release. The obtained results supports and establish that increased drug release is because of small-size and larger surface area of NPs. In conclusion, greater the surface area, higher will be diffusion of drug molecules via different surface sites.

Different kinetic models were studied and can best explain the drug release behavior of formulations at both pH. The model that best fits the release data was evaluated by correlation coefficient (r) value. The correlation coefficient (r) values were used as the criteria to choose the suitable model describing drug release from LPHNPs. The $r^2$ values for different kinetic models at pH 5.4 have been summarized in **Table 2**. The release data from all formulations fitted into Korsemeyer-Peppas equation showed Fickian diffusion($n<0.45$)[21] **(Table2)**.

**-Space for Table 2-**

### 3.7 Stability Study

There were hardly any significant ($p>0.05$) changes observed in particle size, PDI and drug content of LPHNPs upon storage for 3 months. **(Table 3)**

**-Space for Table 3-**

### 3.8 Cell uptake study

Interactions of lipid coated biodegradable NPs with tumor cells are of great interest in tumor-targeted therapies as they can encapsulate and deliver various anti-cancer therapeutics. The relationship with size and cellular uptake and cytotoxicity was evaluated in MCF-7 cells **(Fig. 4A, B and C)**. Uptake of coumarin-6-loaded LPHNPs was evaluated after incubation with MCF-7 cells at 37°C. The coumarin-6-MTX-LPHNPs incubated with MCF-7 cells for 3h observed significant *($p<0.05$)* and rapid internalization, which was corroborated by persistent fluorescence signals

seen even after 3 h when MTX-NPs were co-encapsulated with coumarin-6 **(Fig. 4A)**. This suggests prolonged cell viability and greater efficacy of MTX. The greater internalization seen with F5 formulation led to better cell uptake as compared with other formulations, however, no significant difference (*p>0.05*) in cellular uptake with F3 and F9 formulations was seen. Although all LPHNPs formulations showed significant *(p<0.05) in-vitro* anti-cancer activity compared to MTX because of nano-size and lipid surface of NPs, F5 (prepared by PL- S-100) showed greater anti-cancer activity and cellular uptake. In other words, particles size was inversely related to cellular uptake. Therefore, smaller particles (F5) showed greater uptake as compared to larger particles (F3 and F9) showing lesser uptake. Our results of cellular uptake activity are well supported by the studies reported earlier. [31]The higher uptake seen in F5 is probably due to smaller particle size, in comparison to other formulations showing enhanced permeation and retention (EPR)[23,32,33]. Although, a little is known about the effect of phospholipid and size on phagocytosis of hybrid NPs, we attempted to investigate phospholipid effect on interactions with MCF-7 breast cancer cells. We first compared intracellular uptake of NPs with different lipid based LPHNPs in MCF-7 carcinoma cells using confocal microscopy. Moreover, uptake of NPs was also quantified by recovering NPs from cells and assessing their fluorescence per milligram of total cellular protein contents (data not shown). The quantification results were in agreement with the confocal images **(Fig. 4C)**. We did not see significant difference (*p>0.05*) in the uptake between F3 and F9. As commonly used particle size in tumor targeted systems is ≤ 200 nm, these results imply that particle size has significant *(p<0.05)* impact on the interactions with tumor cells.

**-Space for Figure 4A 4B and 4C-**

### 3. 9 *In vitro* cell cytotoxicity

The cell cytotoxicity was assessed by MTT and IF assay. Toxicity associated with different NPs formulations following incubation with MCF-7 cells for 24, 48 and 72 h was determined **(Fig. 4B)**. Present study is designed to see cell viability, and is plotted against drug concentration with different NPs formulations. We saw concentration dependent reduction in cell viability at given time points with MTX and MTX-LPHNPs. These results suggest that MTX retained its anti-

tumor efficacy even upon loaded onto polymeric NPs and that encapsulation procedure did not have any impact on its anti-tumor potential. Also, MTX loaded into LPHNPs showed better anti-cancer activity compared to that seen with plain MTX. The regression analysis showed same trends in concentration dependent cytotoxicity. Consistent with earlier reports[30], lower $IC_{50}$ of MTX-LPHNPs were determined when compared to free MTX **(Table 4)**. The MTX-LPHNPs showed sustained reduction in cell viability and % age cell survival in comparison to MTX **(Fig. 4B)**. Formulation F5 showed significantly higher *($p<0.01$)* anticancer activity as compared to F3 and F9. The MTX release profile showed that F5 released almost same amount of MTX for 24 h, 48 and 72 h **(Fig. 3 and 4B)**. Briefly, even though same amount of NPs enters tumor cells, real volume of MTX released from NPs is a viable parameter to assess anti-tumor activity. As particle size affects cell cytotoxicity[31], The % viability has been in coherence with drug sensitivity assay ($IC_{50}$) and well supported by the results obtained from immunofluorescence assay (IFA) carried out with Cell Tracker Green CMFDA (5-chloromethylfluorescein diacetate) fluorescent dye (Fig. 4C). The greater number of living/viable cells was seen at higher $IC_{50}$ with all drug-loaded formulations. However, F5-CMFDA (LPHNPs loaded with CMFDA labeled MTX) formulation showed significantly *($p<0.05$)* better anti-cancer efficacy (higher % age of apoptotic and/or lower percentage of surviving tumor population at higher $IC_{50}$) (Fig 4B) as compared to that seen with other formulations. The enhanced and controlled efficacy of LPNHPs suggests higher and sustained drug release with Fickian diffusion at acidic pH showing controlled and enhanced permeation into cells due to their nanosize[34].

**-Space for Figure 4-**

Our findings supports the hypothesis that large size LPHNPs lead to an increase in tumor cell viability. Smaller NPs (<200 nm) can more efficiently escape phagocytosis by induced by macrophages/monocytes in spleen and liver, and therefore enter tumor cells with pace than their larger counterparts. Further, we hypothesize that hydrophilic polyethylene oxide and poly propylene oxide chains of the poloxamer based surfactant may impart hydrophilicity to the NPs surface which may also contributes in evasion of RES clearance. However, further *in vivo*

investigations are warranted to identify effects of nanoparticle size and surface hydrophilicity in biological environments.

## 4. Conclusions and future perspectives

MTX-loaded LPHNPs ranging from 150 to 400 nm were prepared by single step nano-precipitation method. The size-controlled NPs demonstrated that nanoscale particle size has significant *(p<0.05)* impact on tumor cell interactions. Smaller NPs had shown greater tumor cell uptake and toxicities than large size NPs. The size-controlled NPs described here would serve as a useful means to elucidate the role of particle size in an array of NPs-based systems including targeted delivery. The developed methodology opens new avenues for other potent drugs to be loaded onto LPHNPs formulation for sustained delivery in order to address ailments such as cancer, arthritis, psoriasis etc. In perspective, the authors acknowledge that current drug loading needs to be significantly improved to render the hybrid nanoparticle formulation to be clinically useful and safe. Further *in vivo* investigations on biodistribution and anticancer efficacy are warranted to validate the *in vitro* findings.

## 5. Acknowledgements

The authors are grateful for the fellowship (SRF) and grant provided by the CSIR HRDG, New Delhi, India. We acknowledge BASF, Mumbai, India for providing poloxamers. We also acknowledge the AIIMS, New Delhi for HR TEM analysis of NPs.

## References

1. L. Zhang, J. M. Chan, F. X. Gu, J. W. Rhee, A. Z. Wang, A. F. Radovic-Moreno, F. Alexis, R. Langer and O. C. Farokhzad, *ACS Nano.*, 2008, **2**, 1696-1702. .
2. K. Hadinoto, A. Sundaresan and W. S. Cheow, *Eur J Pharm Biopharm.*, 2013, **85**, 427-443.
3. R. H. Fang, S. Aryal, C. M. Hu and L. Zhang, *Langmuir*, 2010, **26**, 16958-16962. .
4. W. S. Cheow and K. Hadinoto, *Colloids Surf B Biointerfaces*, 2011, **85**, 214- 220. .
5. C. M. Hu, S. Kaushal, H. S. TranCao, S. Aryal, M. Sartor, S. Esener, M. Bouvet and L. Zhang, *Mol Pharm*, 2010, **7**, 914-920. .
6. A. Jain, A. Jain, N. K. Garg, R. K. Tyagi, B. Singh, O. P. Katare, T. J. Webstere and V. Soni, *Acta Biomater.*, 2015. doi:10.1016/j.actbio.2015.06.027
7. S. Vezmar, A. Becker, U. Bode and U. Jaehde, *Chemotherapy.*, 2003, **49**, 92-104.

8. D. Banerjee, P. Mayer-Kuckuk, G. Capiaux, T. Budak-Alpdogan, R. Gorlick and J. R. Bertino, *Biochim Biophys Acta.*, 2002, **1587**, 164-173.

9. L. Battaglia, L. Serpe, E. Muntoni, G. Zara, M. Trotta and M. Gallarate, *Nanomed*, 2011, **6**, 1561-1573. .

10. M. F. Pinto, C. C. Moura, C. Nunes, M. A. Segundo, S. A. Costa Lima and S. Reis, *Int J Phamr*, 2014, **477**, 519-526.

11. M. Afshari, K. Derakhshandeh and L. Hosseinzadeh, *J Microencapsul*, 2014, **31**, 239-245.

12. X. Yang, Q. Zhang, Y. Wang, H. Chena, H. Zhang, F. Gao and L. Liu, *Colloids Surf B Biointerfaces*, 2008, **61**, 125-131.

13. P. Srisuka, P. Thongnopnuab, U. Raktanonchaic and S. Kanokpanont, *Int J Phamr*, 2012, **427**, 426– 434.

14. V. Dubey, D. Mishra, T. Dutta, M. Nahar, D. K. Saraf and N. K. Jain, *J Controlled Release*, 2007, **123**, 148-154.

15. N. Maurer, D. B. Fenske and P. R. Cullis, *Expert Opin Biol Ther.*, 2001, **1**, 923-947.

16. X. Zhao, F. Li, Y. Li, H. Wang, H. Ren, J. Chen, G. Nie and J. Hao, *Biomaterials*, 2015, **46:13-25.**

17. J. Shi, Y. Xu, X. Xu, X. Zhu, E. Pridgen, J. Wu, A. R. Votruba, A. Swami, B. R. Zetter and O. C. Farokhzad, *Nanomedicine*, 2015, **10**, 897-900.

18. Y. Yi, Y. Li, H. Wu, M. Jia, X. Yang, H. Wei, J. Lin, S. Wu, Y. Huang, Z. Hou and L. Xie, *Nanoscale Res Lett*, 2014, **9**, 560.

19. Jain, S.; Chauhan, D. S.; Jain, A. K.; Swarnakar, N. K.; Harde, H.; Mahajan, R. R.; Kumar, D.; Valvi, P. K.; Das, M.; Datir, S. R.; Thanki, K. A universal step-wise freeze drying process for lyophilization of pharmaceutical products. *Indian Patent* Application No 2559/DEL/201*1*.

20. B. Amarji, N. K. Garg, S. Singh and O. P. Katare, *J Drug Target*, 2015, **DOI:10.3109/1061186X.2015.1058804**.

21. P. Costa and J. M. Sousa Lobo, *Eur J Pharm Sci.*, 2001, **13**, 123-133.

22. A. K. Jain, K. Thanki and S. Jain, *Mol Pharm*, 2013, **10**, 3459-3474.

23. N. K. Garg, P. Dwivedi, C. Campbell and R. K. Tyagi, *Eur J Pharm Sci*, 2012, **47**, 1006-1014.

24. P. Ekambaram and H. S. Abdul, *J Young Pharm*, 2011, **3**, 216-220.

25. Y. Y. Yang, T. S. Chung and N. P. Ng, *Biomaterials*, 2001, **22**, 231-241.

26. Q. Yang and G. Owusu-Ababio, *Drug Dev Ind Pharm.*, 2000, **26**, 61-70.

27. Y. Y. Yang, T. S. Chung, X. L. Bai and W. K. Chan, *Chem Eng Sci*, 2000, **55**, 2223-2236.

28. S. M. Moghimi, A. C. Hunter and J. C. Murray, *Pharmacol Rev*, 2001, **53**, 283-318.

29. M. J. Sailor and J. H. Park, *Adv Mater*, 2012, **24**, 3779-3802.

30. M. Das, R. P. Singh, S. R. Datir and S. Jain, *Bioconjug Chem*, 2013, **24**, 626-639.

31. J. S. Choi, J. Cao, M. Naeem, J. Noh, N. Hasan, H. K. Choi and J. W. Yoo, *Colloids Surf B Biointerfaces*, 2014, **122:545-51.**

32. K. Greish, *J Drug Target*, 2007, **15**, 457-464.

33. A. Jain, P. Kesharwani, N. K. Garg, J. A., J. S.A., A. K. Jain, P. Nirbhavane, R. Ghanghoria, R. K. Tyagi and O. P. Katare, *Colloids and Surfaces B: Biointerfaces*, 2015., doi:10.1016/j.colsurfb.2015.06.027.

34. A. K. Jain, N. K. Swarnakar, C. Godugu, R. P. Singh and S. Jain, *Biomaterials*, 2011, **32**, 503-515.

| **Figure legends** | |
|---|---|
| **Scheme 1** | Schematic illustration shows the development of self-assembled lipid polymer hybrid nanoparticles (LPHNPs). |
| **Figure 1** | Effect of a) surfactant and b) Polymer Lipid ratio on size and % age entrapment efficiency of NPs. Data are expressed as mean ± SD (n=6). The F5 shows significant *(p<0.001) lower particle size with significant (p<0.001) higher entrapment as compared to that seen with F3 and F9* at all surfactant concentration & lipid-polymer ratio. |
| **Figure 2** | Characterizations of LPHNPs (F5) in combination with Phospholipids S 100<br>Figure 1B: TEM images of MTX loaded PCL NPs (a) and LPHNPs (b)<br>Figure 1C: (a) FT-IR overlay spectra of, MTX, Plain LPHNPs, MTX loaded LPHNPs<br>(b)XRD profiles of MTX, LPHNPs and MTX loaded LPHNPs |
| **Figure 3** | *In vitro* drug release of LPHNPs at pH 7.4 and 5.4. Data are expressed as mean ± SD (n=6) |
| **Figure 4A** | Cell uptake study of selected LPHNPs (F3, F5, F9) using MCF-7cells, a) Coumarine-6 LPHNPs uptake by cells b) Overlay of figure a and c c) Cells without treatment of coumarine-6 cells. d) Magnified view of overlay. (e) Line series analysis of fig b- white line depicting normal cells, while green line depicting fluorescent cells. The F5 showing significant *(p<0.05)* cell uptake in comparison to F5 & F9. |
| **Figure 4B** | Cell viability assay of different LPHNPs formulations. Data are expressed as mean ± SD (n=6). The F5 shows significant *(p<0.05)* decrease in cell viability as compared to that seen with plain MTX |
| **Figure 4C** | Immunofluorescence assay performed with MCF-7 cells loaded with plane MTX and différent LPHNPs formulations. a) CMFDA labeled methothrexate, b) CMFDA-labeled F3, c) CMFDA-labeled F5 and d) CMFDA-labeled F9. The % age of viable cells decreased when incubated for 24, 48 and 72h. 200K cells were cytospine and fixed with 4% paraformaldehyde. The cells cytospine onto slides were then labeled with CMFDA (10µM) following manufacturer's recommendations (life technologies). The present results were shown consistency in two independent experiments. The F5 showing significant *(p<0.05)* cell uptake as compared to that observed with F5 & F9. |
| **Table legends** | |
| **Table 1** | Effect of lipids and surfactants on LPHNPs formulation and characterization. Data are expressed as mean ± SD (n=6). The F5 shows highly significant *(p<0.01)* effect on particle size & entrapment when compared with F5 and F9. |
| **Table 2** | Different drug release models for *in vitro* release study. Data are expressed as mean ±SD (n=6) |
| **Table 3** | Stability date of the MTX formulation after 3 months of studies. Data are expressed as mean ± SD (n=6) |
| **Table 4** | MTT viability assay of different formulations. Data are expressed as mean ±SD (n=6). The F5 shows greater *(p<0.05, highly significant)* anti-cancer activity compared in comparison to F5, F9, and plain MTX after each time interval. |
| **Supporting Information** | |

| SI Table 1 | A) Effect of surfactant concentration on size and EE of LPHNPs. Data are expressed as mean ± SD (n=6)<br>B) Effect of Lipid to polymer ratio on characteristics of LPHNPs. Data are expressed as mean ± SD (n=6) |
|---|---|

**Table 1:**

| S. No. | Lipid | Surfactant used | Zeta potential (mV) | Particle size (nm) | PDI | EE (%) |
|---|---|---|---|---|---|---|
| F1 | PL- 90G | Tween 80 | -14.78 ± 2.1 | 351 ± 17.8 | 0.281± 0.01 | 68.20±2.1 |
| F2 | | Kolliphor® P 407 | -13.38 ± 1.1 | 311 ± 15.4 | 0.275± 0.01 | 74.29± 1.7 |
| **F3** | | Lutrol® F-87 | -13.67± 1.9 | 295.8±5.6 | 0.234± 0.02 | 78.8 ± 2.8 |
| F4 | | PVA | -16.8 ± 2.2 | 241.5 ± 11.5 | 0.218± 0.02 | 69.90±3.2 |
| F5 | PL-S100 | Lutrol® F-87 | -15.4±1.1 | 171.06± 8.9 | 0.157± 0.02 | 89.9± 2.6 |
| F6 | | Tween 80 | -16.2 ± 2.7 | 222.6 ± 11.5 | 0.211± 0.02 | 70.6±2.4 |
| F7 | | Kolliphor® P 407 | -15.7±2.5 | 233.4 ± 13.3 | 0.284± 0.01 | 74.3±3.6 |
| F8 | | PVA | -11.7± 1.8 | 228.5 ± 12.7 | 0.312± 0.02 | 71.68±2.8 |
| F9 | L-SPC-3 | Lutrol® F-87 | -14.8± 2.2 | 254.5± 11.2 | 0.223± 0.03 | 82.23 ± 3.2 |
| F10 | | Tween 80 | -13.6± 3.1 | 322.4 ± 10.8 | 0.354± 0.02 | 64.89 ± 2.9 |
| F11 | | Kolliphor® P 407 | -14.21± 2.8 | 330.2± 12.7 | 0.302± 0.02 | 72.65 ± 2.8 |
| F12 | | PVA | -12.5± 1.9 | 330.6± 11.6 | 0.295± 0.02 | 67.54 ± 3.3 |
| Note: Lipid: Polymer ratio was kept at 1:2, while surfactant was kept constant 0.5% w/v in all formulation | | | | | | |

**Table 2:**

| Formulations | Storage condition | Time | Zeta potential (mV) | Particle size (nm) | PDI | Percentage of drug (assay) |
|---|---|---|---|---|---|---|
| F3 | | Initial | -13.67 ± 0.9 | 295.8 ± 5.6 | 0.34 ± 0.02 | 98.8 ± 2 |
| | 2-8°C | After 3 months | -13.38 ± 0.8 | 298 ± 5.4 | 0.25 ± 0.01 | 97.29 ± 1.7 |
| | 25±2°C/60±5%RH | | -13.67 ± 0.9 | 299.8 ± 5.6 | 0.34 ± 0.02 | 97.2 ± 2.8 |
| | 40±2°C/75±5%RH | | -16.8 ± 0.8 | 302.5 ± 4.5 | 0.38 ± 0.02 | 99.79 ± 3.2 |
| F5 | | Initial | -15.4 ± 1.1 | 171.06 ± 8.9 | 0.17 ± 0.02 | 98.9 ± 2.6 |
| | 2-8°C | After 3 months | -16.2 ± 0.7 | 178.6 ± 4.5 | 0.21 ± 0.02 | 97.66 ± 2.4 |
| | 25±2°C/60±5%RH | | -15.7 ± 0.7 | 183.4 ± 5.3 | 0.34 ± 0.01 | 96.98 ± 3.6 |
| | 40±2°C/75±5%RH | | -14.7 ± 0.6 | 184.5 ± 6.7 | 0.22 ± 0.02 | 96.88 ± 2.8 |
| F9 | | Initial | -14.8 ± 0.3 | 254.5 ± 11.2 | 0.23 ± 0.03 | 99.23 ± 3.2 |
| | 2-8°C | After 3 months | -13.6 ± 0.6 | 256.4 ± 8.8 | 0.24 ± 0.02 | 98.89 ± 2.9 |
| | 25±2°C/60±5%RH | | -13.21 ± 0.8 | 260.2 ± 5.7 | 0.12 ± 0.02 | 98.05 ± 2.8 |
| | 40±2°C/75±5%RH | | -13.5 ± 1.9 | 264.6 ± 4.6 | 0.15 ± 0.02 | 97.08 ± 3.3 |

**Table 3:**

| Formulation | Drug Release Models ($r^2$) at pH 5.4 | | | | | |
|---|---|---|---|---|---|---|
| | Zero order | First order | Higuchi | Hixon Crowell | korsmeyerpeppas | |
| | | | | | $r^2$ | n |
| **F3** | 0.8735 | 0.673 | 0.9817 | 0.9335 | 0.9946 | 0.30 |
| **F5** | 0.8869 | 0.6642 | 0.9892 | 0.9362 | 0.9964 | 0.386 |
| **F9** | 0.8898 | 0.7171 | 0.8478 | 0.939 | 0.996 | 0.309 |

**Table 4:**

| Formulations | $IC_{50}$(µg/mL) | | |
|---|---|---|---|
| | 24 h | 48 h | 72 h |
| **MTX** | 10.39 ± 0.83 | 6.74 ± 0.41 | 4.61± 0.01 |
| **MTX-F3** | 8.54 ± 0.72 | 4.83 ± 0.03 | 3.89 ± 0.21 |
| **MTX-F5** | 6.97± 0.54 | 3.45 ± 0.04 | 2.73 ± 0.65 |
| **MTX-F9** | 8.21 ± 0.65 | 4.64± 0.03 | 3.75 ± 0.81 |

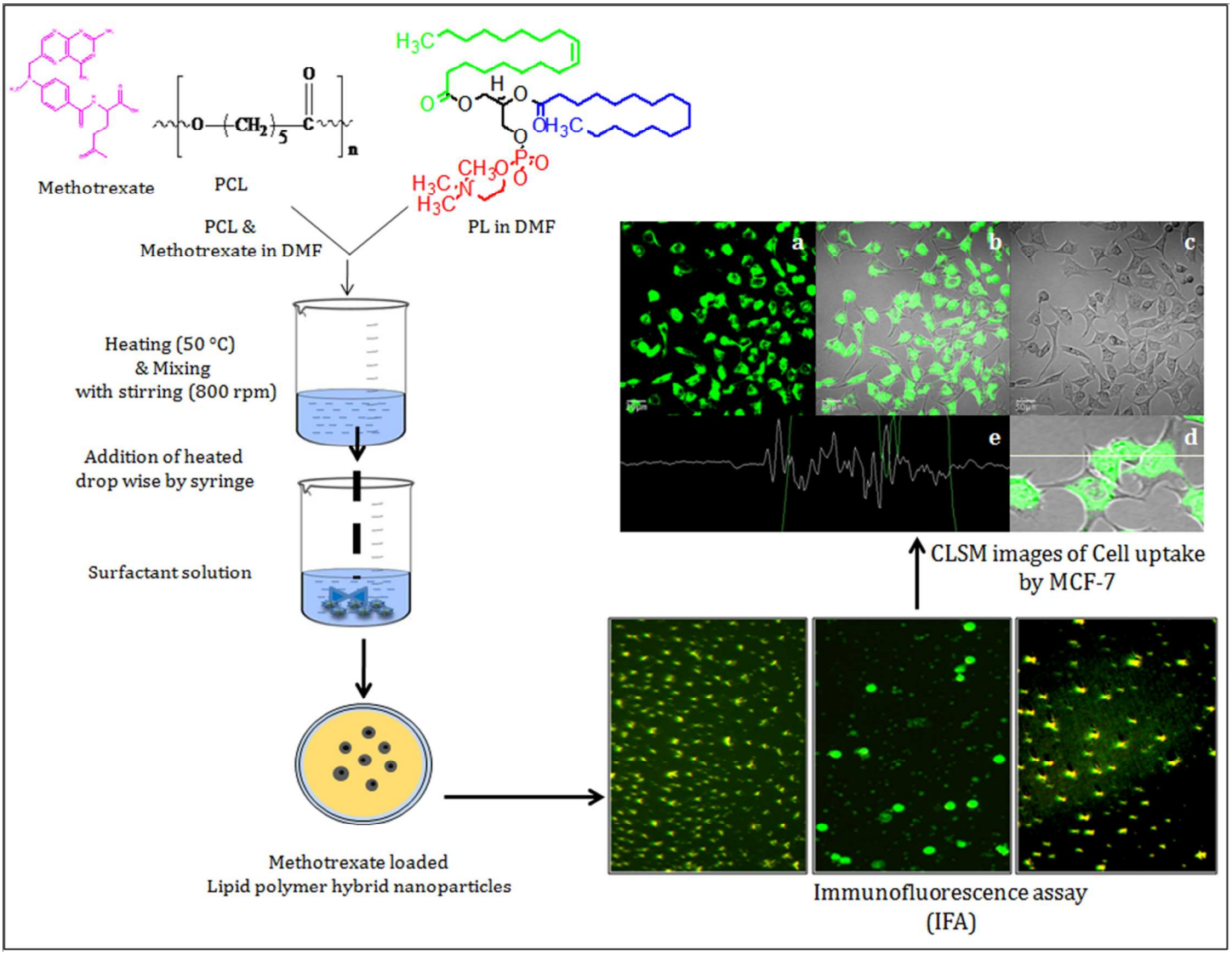


**Graphical Abstract**

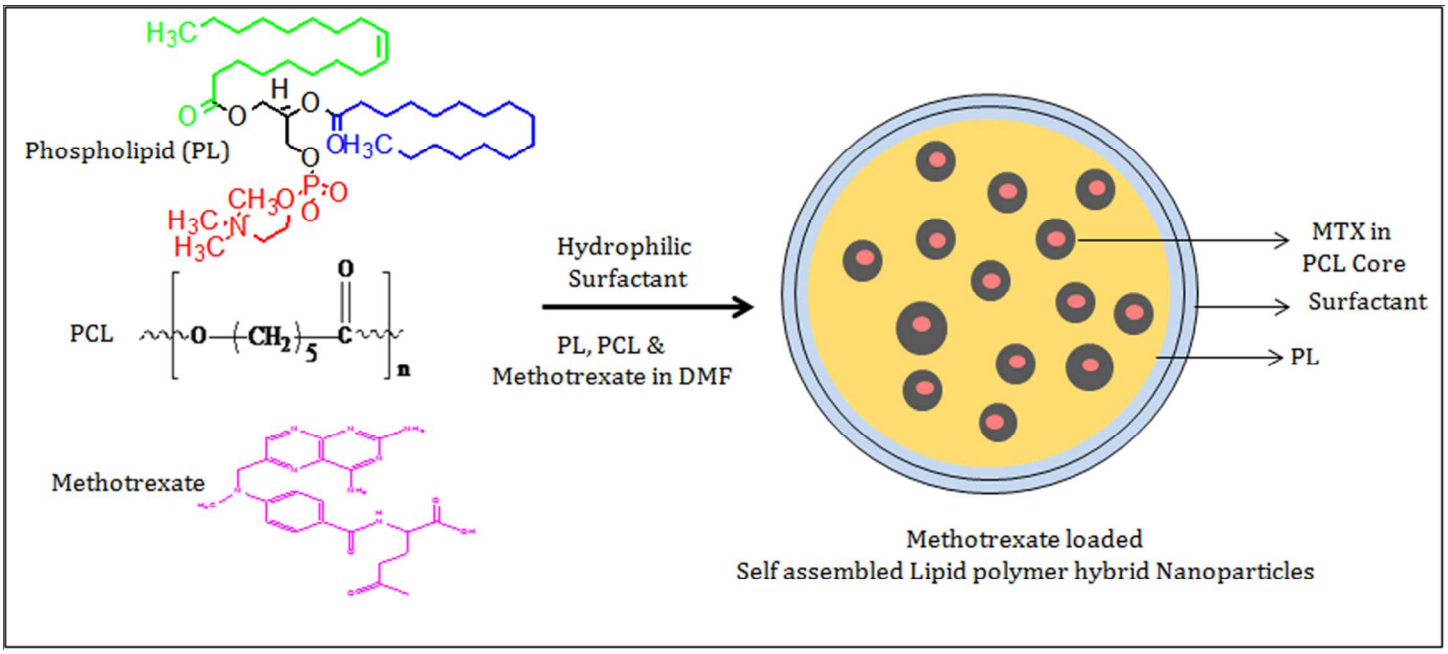


**Scheme 1**

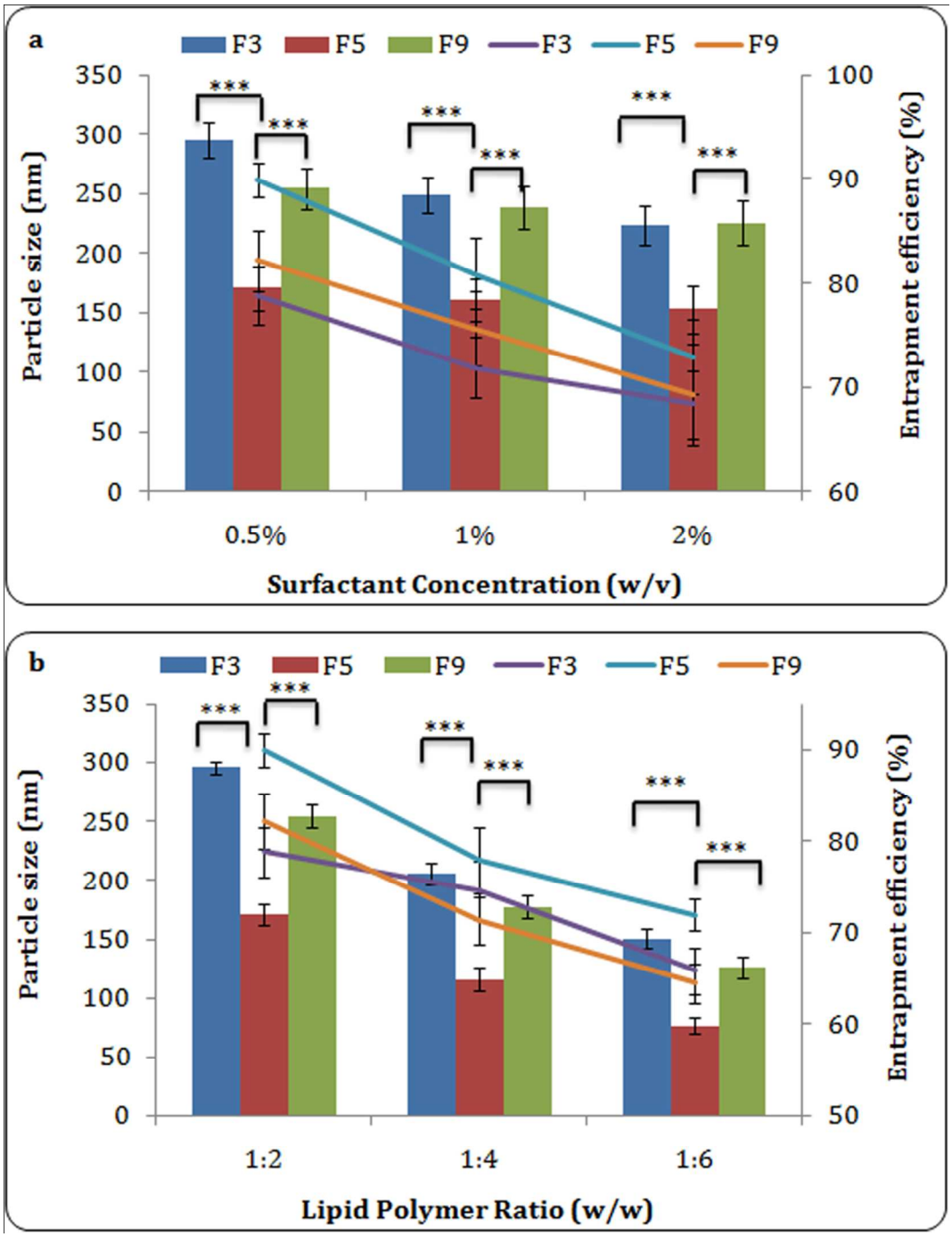


**Figure 1**

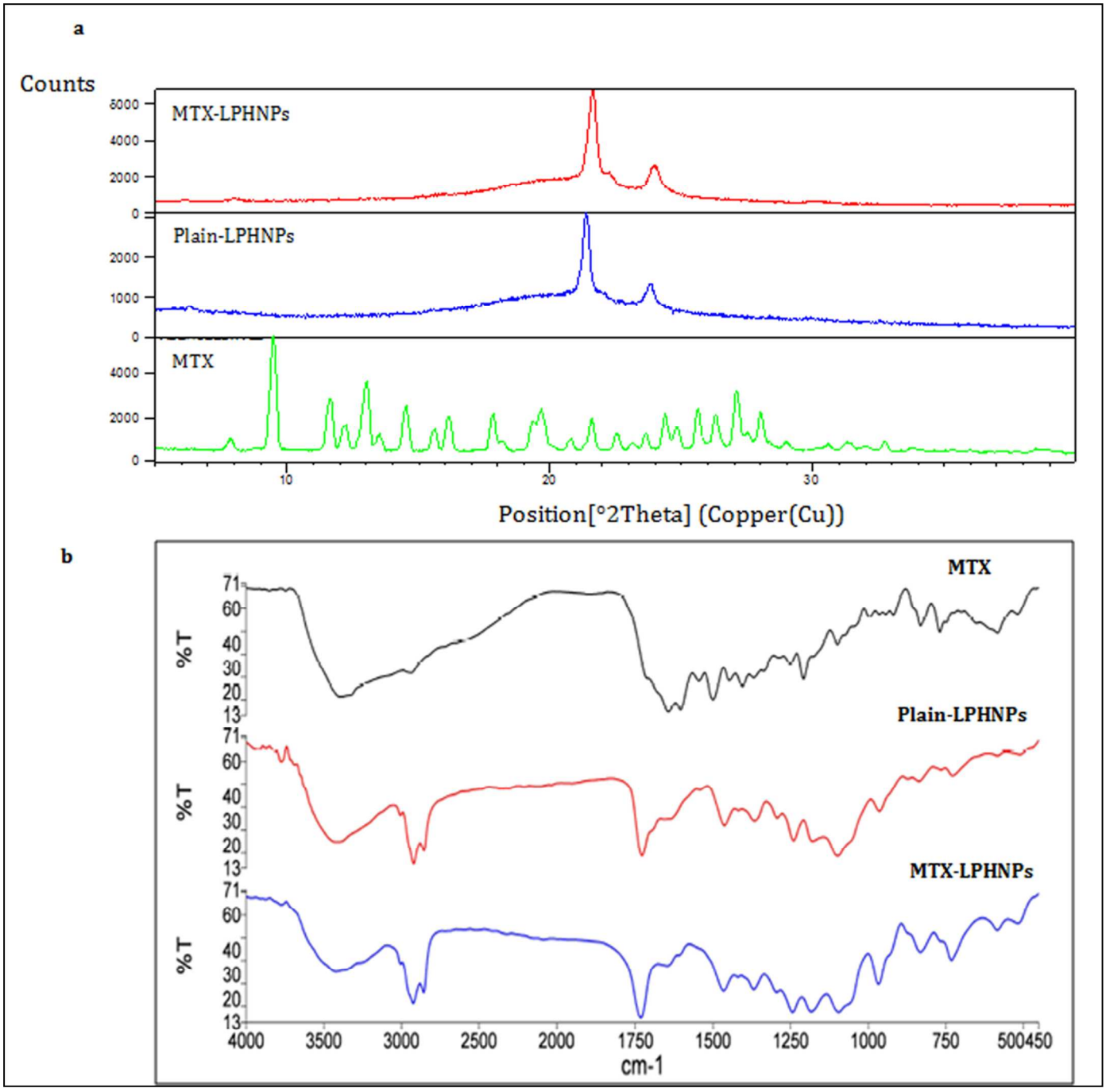


**Figure 2A**

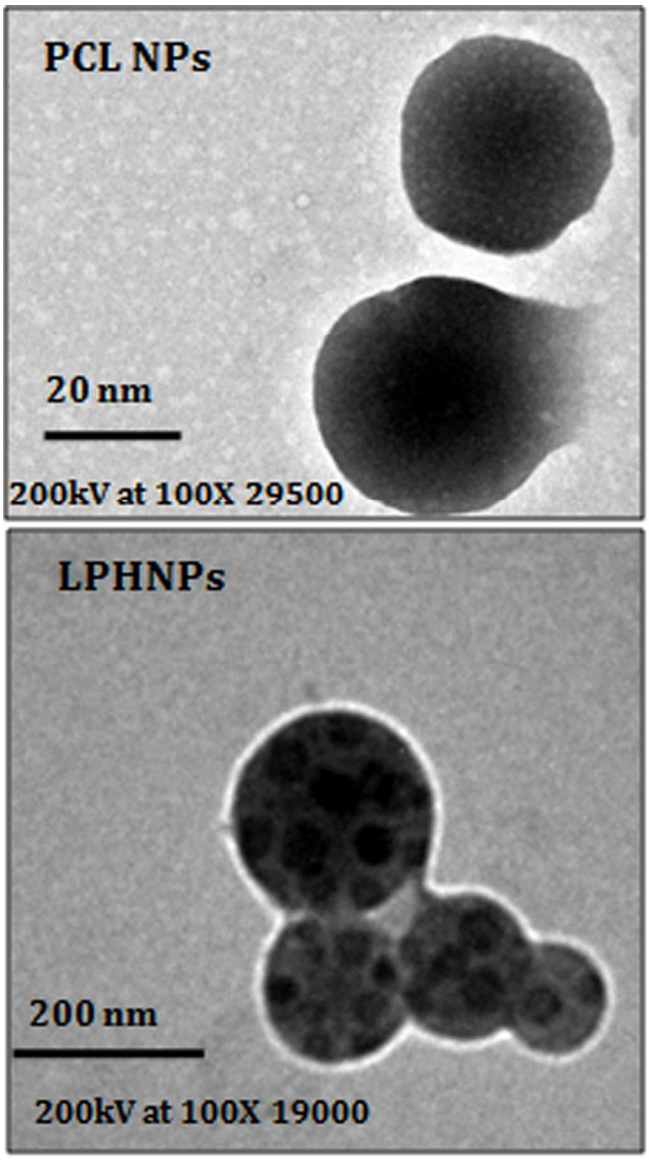


**Figure 2B**

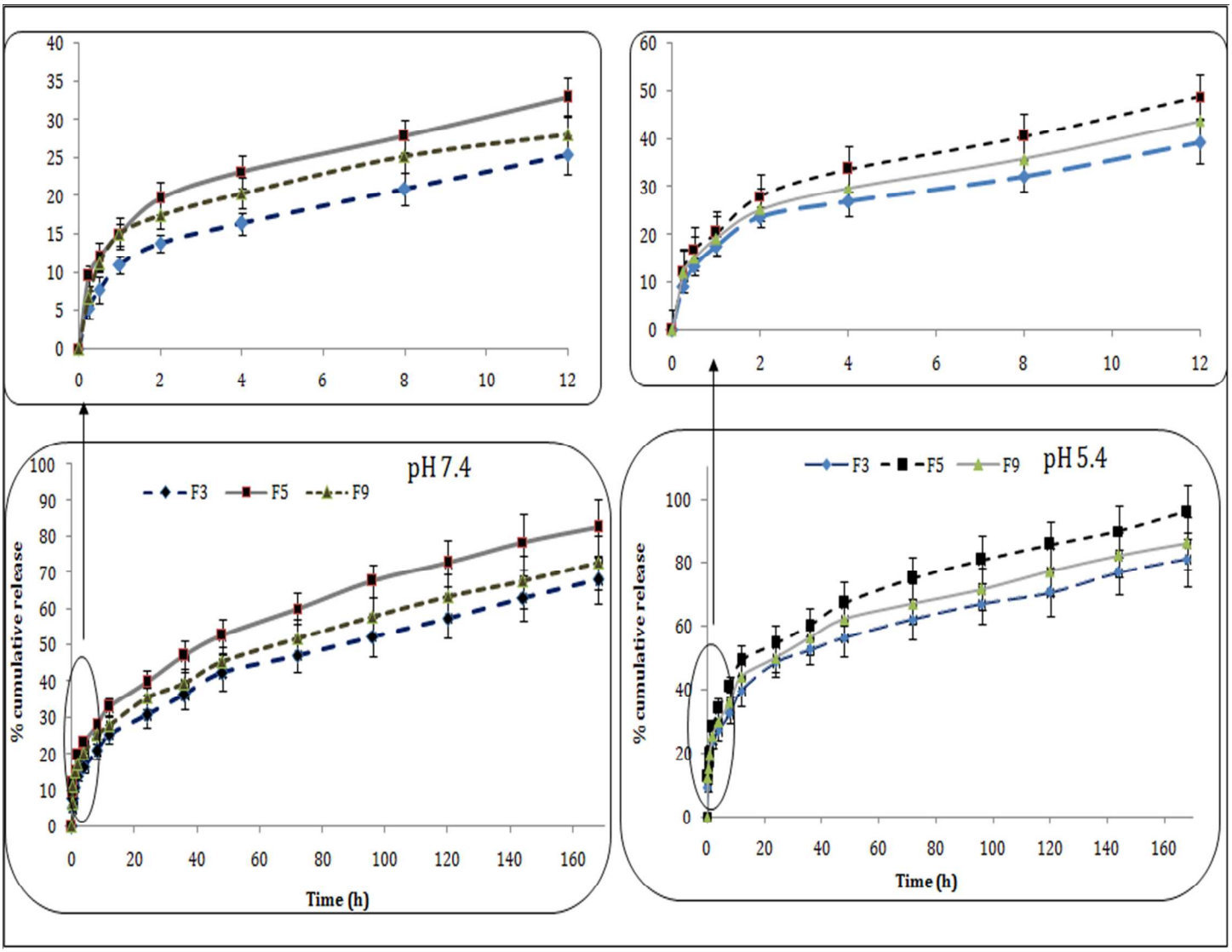


**Figure 3**

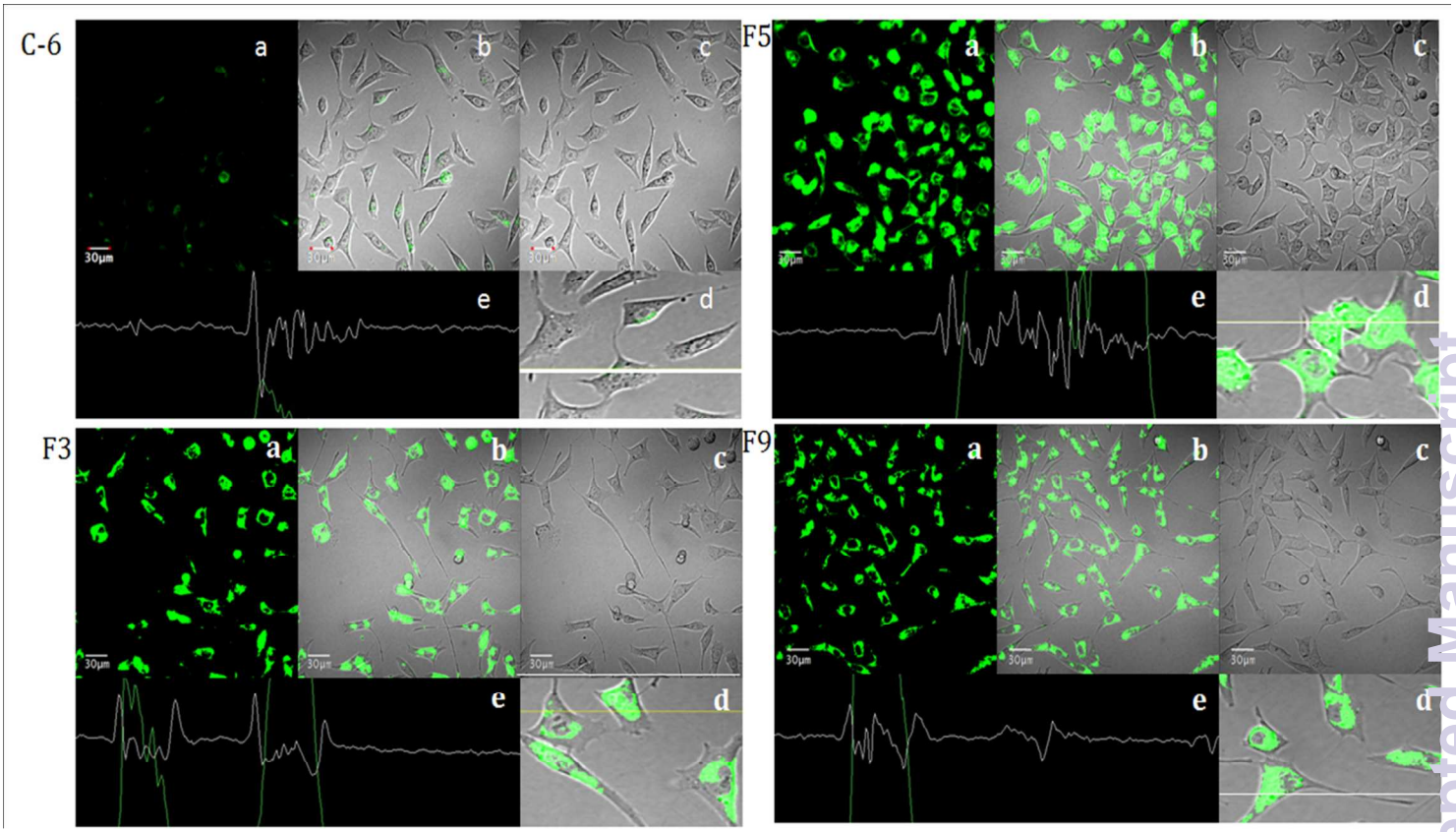


**Figure 4A**

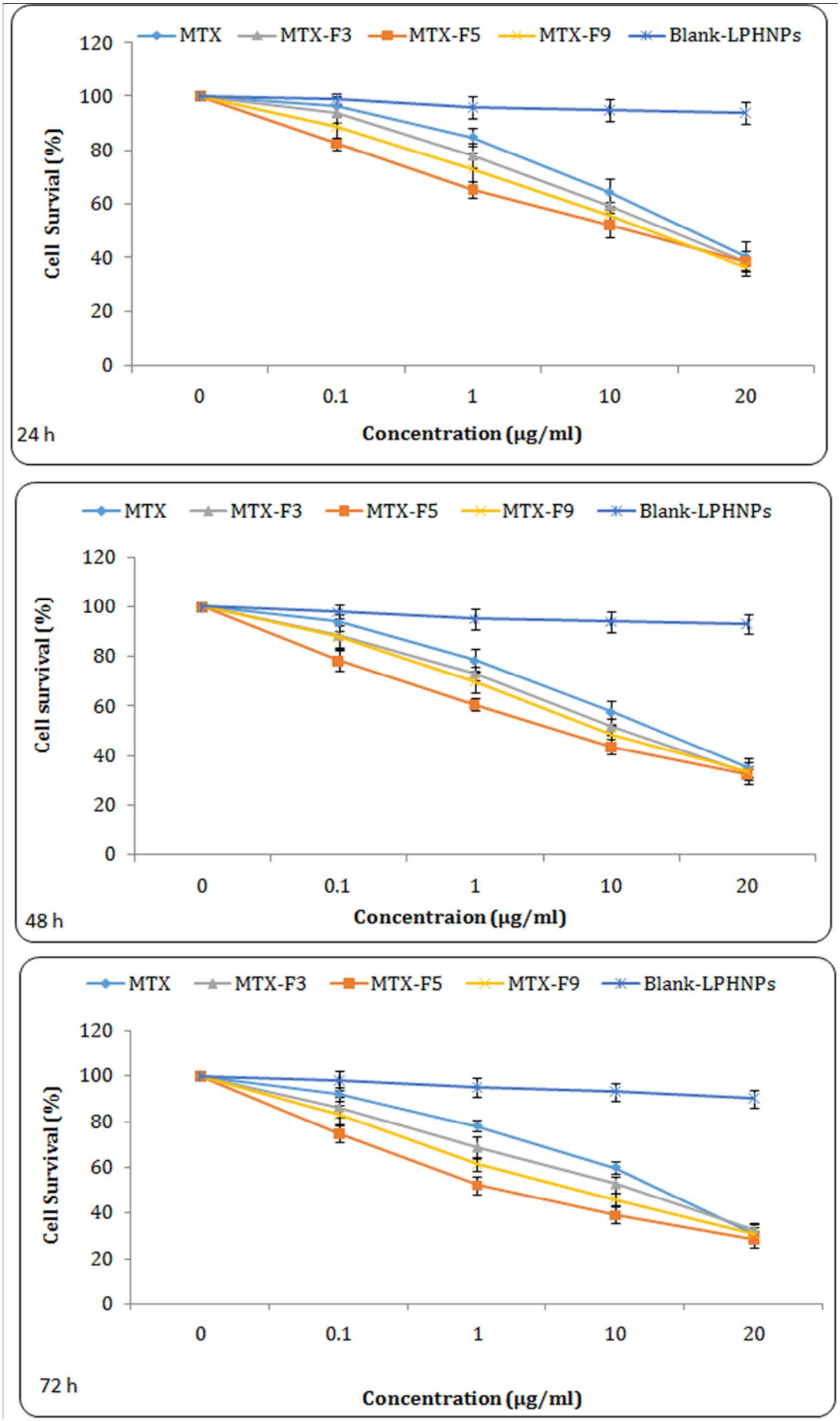


Figure 4B

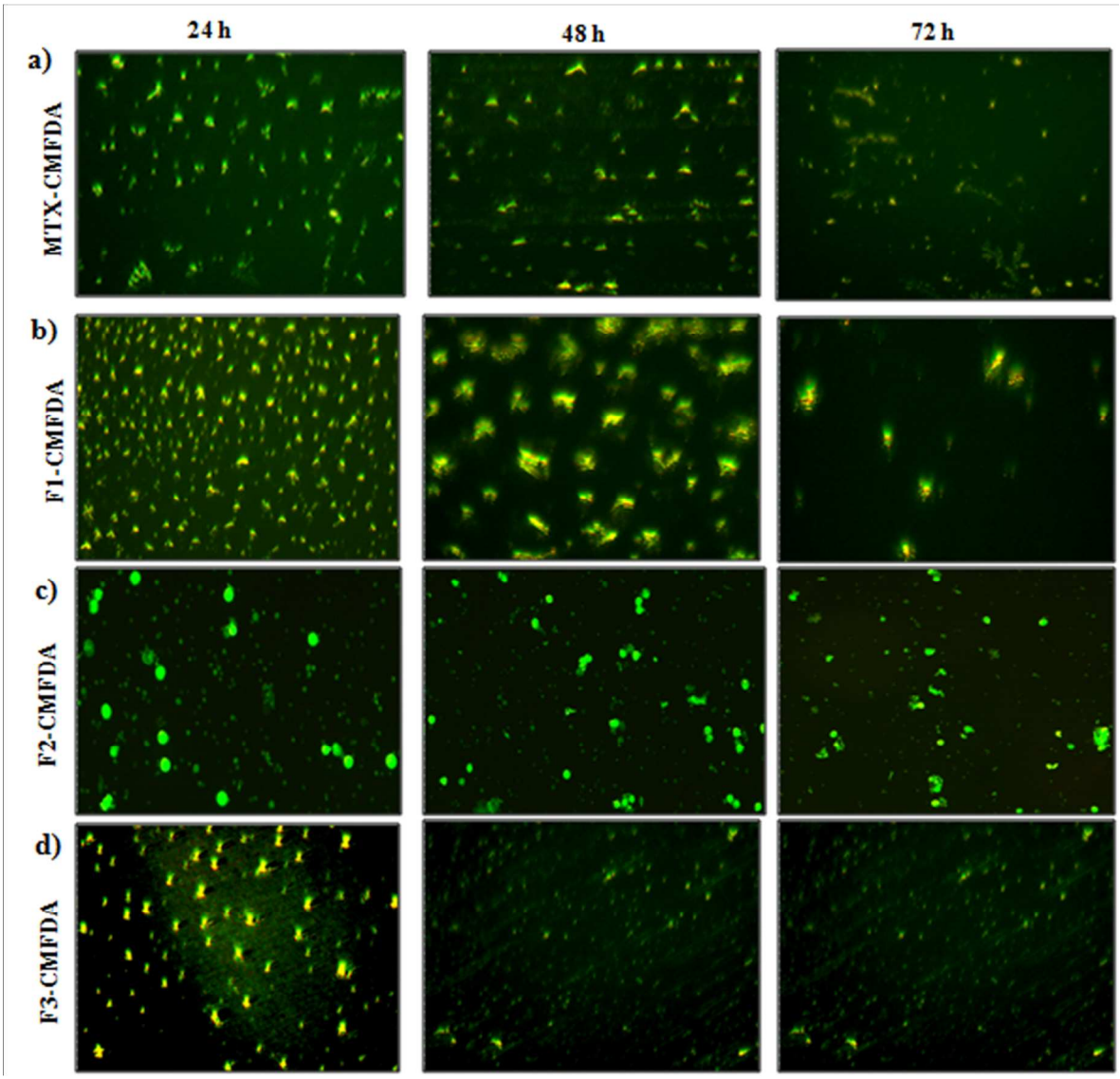


Figure 4C